Synthesis and applications of CdSe nano-tetrapods in hybrid photovoltaic devices*

Lijuan Zhao[1,†] and Linfeng Hu[2,‡]

[1]*Department of Physics, Donghua University, Shanghai 201620, China;*
[2]*Department of Materials Science, Fudan University, Shanghai 200433, China*

Abstract: Tetrapod-shaped nanocrystals have attracted increasing interest for optoelectronic applications in recent years due to their rich morphologies. With unique properties such as a direct band-gap and excellent photoelectrical characteristics, CdSe nano-tetrapods are promising nanostructures for applications in such fields as photodetectors, field emitters, and photovoltaic devices. This review mainly describes the remarkable progress made in synthesis and hybrid photovoltaic applications of CdSe nano-tetrapods over the last few years. In particular, the "blinking" effect observed from these nano-tetrapods in chloroform solution is highlighted. This overview covers the current state of the art as well as an outlook on possibilities and limitations.

Keywords: CdSe; hybrid photovoltaic applications; nano-tetrapods; synthesis.

INTRODUCTION

The tetrapod-shaped nanocrystal, which consists of a zinc-blende core with four {111} facets, each projecting a wurtzite rod terminated with the (000) facet, can potentially give rise to a variety of interesting mechanical, electrical, and optical properties. For example, due to their three-dimensional character, tetrapods may be important alternatives to fibers and rods as additives for mechanical reinforcement of polymers [1]. Tetrapods can also serve as a very interesting building block for preparing superstructures, especially three-dimensional ones [2].

Those CdSe nanocrystals which have a wide band-gap favoring absorption over a wide range of the visible spectrum have been proposed as working elements for nanotransistors [3], electrochromic materials [4], optoelectronic devices [5], and charge-coupling devices [6]. In particular, three-dimensional CdSe nano-tetrapods have obvious potential advantages in photovoltaic devices [7,8] because their shape makes it impossible for them to lie flat within the film. Up to now, tetrapod-shaped crystals with dimensions on the nanometer and micrometer scale have been synthesized for a variety of II–VI semiconductors including ZnO [9,10], CdS [11–13], CdTe [1,14], ZnS [15–17], and CdSe [18,19].

CdTe nano-tetrapods have previously been synthesized using CdO as cadmium precursor in an oleic acid (OA)-trioctylphosphine (TOP) system or in a mixture of surfactant of octadecylphosphinic acid (ODPA) and the trioctylphosphine oxide (TOPO)-TOP system, respectively. It has been shown that it is possible to obtain a high yield of colloidal CdTe tetrapods with well-controlled nanoscale dimensions [14]. On the other hand, only very low yields of colloidal CdSe nano-tetrapods are observed in the synthesis of CdSe nanorods using CdO as the cadmium precursor in a surfactant mixture of tetra-

[†]Fax: +86-21-67792085; E-mail: ljzhao@dhu.edu.cn
[‡]Corresponding author

decylphosphonic acid (TDPA) and the TOPO-TOP system. In this review, the methods of synthesis of CdSe nano-tetrapods will first be presented. Then, the "blinking" effect observed for CdSe nano-tetrapods in chloroform solution and the hybrid photovoltaic device based on CdSe nano-tetrapods will be discussed. The review concludes with an outlook of possibilities and limitations in this area.

SYNTHESIS OF CdSe NANO-TETRAPODS

Several methods of growth have been developed for nano-tetrapods. They can be roughly subclassified into methods which produce powders or agglomerated nanocrystals, for example, through chemical vapor deposition for ZnO nano-tetrapods, and methods resulting in colloidal nanocrystals, including an organo-metallic approach and micellar synthesis. CdSe nano-tetrapods are often prepared by an organo-metallic approach. In addition, many recently published synthetic methods cannot readily be categorized as above, because they utilize an approach based upon methodological hybridization.

As a breakthrough in this field, Alivisatos, Peng, and their co-workers synthesized a series of nearly monodispersed II–VI group nano-semiconductors using different cadmium precursors in TOPO [18,20]. Peng et al. used nonorganic CdO and Se powder as precursors, TOPO and ODPA as the coordinating surfactant and TOP as solvent for CdO and Se, respectively, to synthesize CdSe nanocrystals. They found that by simply increasing the precursor concentration at 300 °C, the morphology of CdSe nanocrystals varied from short rods to long rods, and then to branched ones. It is difficult to completely exclude the nanorods and multiarmed nanocrystals during the growth of CdSe nano-tetrapods [18]. The reason is that one of the key parameters for achieving tetrapod growth is the energy difference between the wurtzite and the zinc-blende structures, which determines the temperature range in which one structure can be preferred during nucleation and the other during growth. In the case of CdSe, the energy difference is only a few millielectronvolts per atom, and it is difficult to isolate controllably the growth of one phase at a time [1].

High-yield CdSe nano-tetrapods can be obtained when OA is used as surfactant and proton acid is added in cadmium precursor at relatively low growth temperature (180 °C) [21]. The resulting products were shown to be spherical CdSe nanocrystals when no proton acid was added. It is believed that the proton acid plays the key role in the growth of CdSe tetrapods. The effect of acidic environment in the reaction system is to initiate the growth of zinc blende core and influence the growth rates of different crystal facets so as to induce anisotropic growth of CdSe nanocrystals. Firstly, proton acidic environment induces the zinc blende nuclei, and then the proton (H^+) may passivate those facets such as {110}, except the four equivalent {111} facets. As a result, the growth can only continue on the four {111} facets. Finally, tetrapod-shaped CdSe nanocrystals can be synthesized in high yield by controlling the proton acidic circumstance of the reaction system.

Wong's group used cetyltrimethylammonium bromide (CTAB) as a coligand to synthesize CdSe nanocrystals at a synthesis temperature of 160 °C [22]. CdO, Se powder, OA, and TOP are used as precursors. 1-Octadecene (ODE) or the heat transfer fluids (HTFs) such as therminol 66 (T66), therminol VP-1 (TVP1), diphenyl oxide (DPO), or biphenyl (BP) is chosen as solvent. It is found that in all phenylated solvents except ODE, spherical nanoparticles are formed at early times, which become tetrapod-shaped with synthesis time, while with ODE, tetrapods are observed at all times, as indicated in Fig. 1. The maximum yield of tetrapods in ODE is 86 %, which is much higher than that of other solvents. Although the growth of tetrapods in ODE is faster than in the other solvents, the ratio of arm thickness and length is nearly the same for all solvent types. The use of HTFs can provide an alternative path toward production-scale quantities of CdSe nano-tetrapods and tetrapods of other compositions.
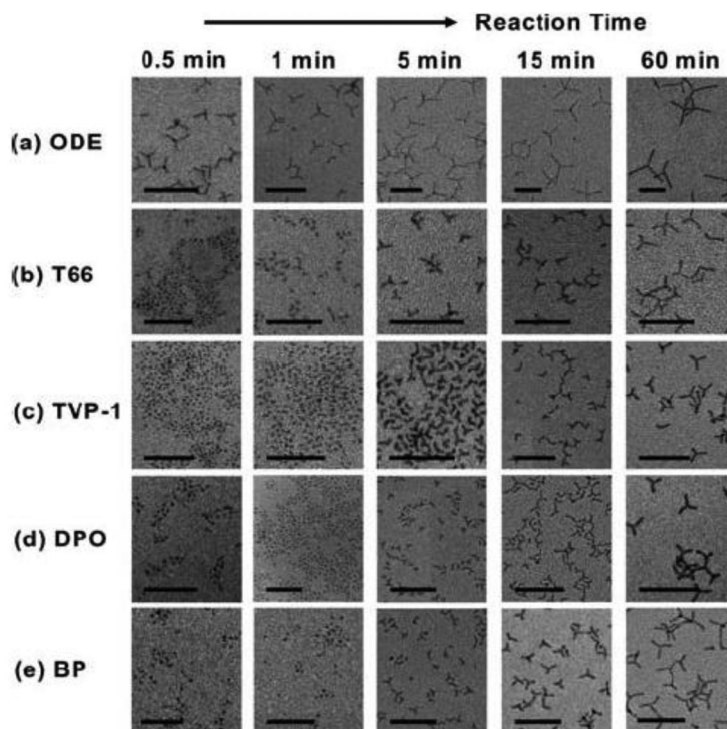
Fig. 1 TEM images of CdSe nano-tetrapods synthesized at the given reaction time in (a) ODE, (b) T66, (c) TVP1, (d) DPO, and (e) BP solvents (injection at 190 °C and growth at 160 °C). Scale bar: 50 nm. Reproduced from [22]. Copyright © 2010, the Royal Society of Chemistry.

Recently, Liu and co-workers explored the surfactant-free recipes for the synthesis of CdSe nanocrystals at a relatively low temperature [23]. Dot-, rod-, tetrapod-, and sphere-shaped CdSe nanocrystals are prepared with TOPO as a nonequilibrium solvent and trioctylphosphine selenide (TOPSe) and cadmium carboxylates such as cadmium laurate $[Cd(C_{12}H_{23}O_2)_2]$, cadmium myristate $[Cd(C_{14}H_{27}O_2)_2]$, cadmium palmitate $[Cd(C_{16}H_{31}O_2)_2]$, and cadmium stearate $[Cd(C_{18}H_{35}O_2)_2]$ as Se and Cd precursors, respectively. It is found that the reaction temperature, monomer concentration, and cadmium precursor have large effects on the morphology of CdSe nanocrystals. When cadmium myristate is used for the TOPSe injection at a high concentration of 2.4 mmol ml^{-1}, tetrapod CdSe nanocrystals can be synthesized at 240 °C. The tetrapod selectivity is up to 85 % for a statistical number of 100. The formation of CdSe nanocrystals takes a very short time, and the nanocrystals grow larger with increasing reaction time. The small tetrapods are found at about 3 min after the injection while the nanocrystals almost stop to grow larger within 10 min as indicated in Fig. 2, which shows the transmission electron microscopy (TEM) images and UV and photoluminescence (PL) spectra of CdSe tetrapods with different reaction time. It is believed that the myristic acid formed in situ could be strongly absorbed on the CdSe primary particles and facilitate the anisotropy growth.
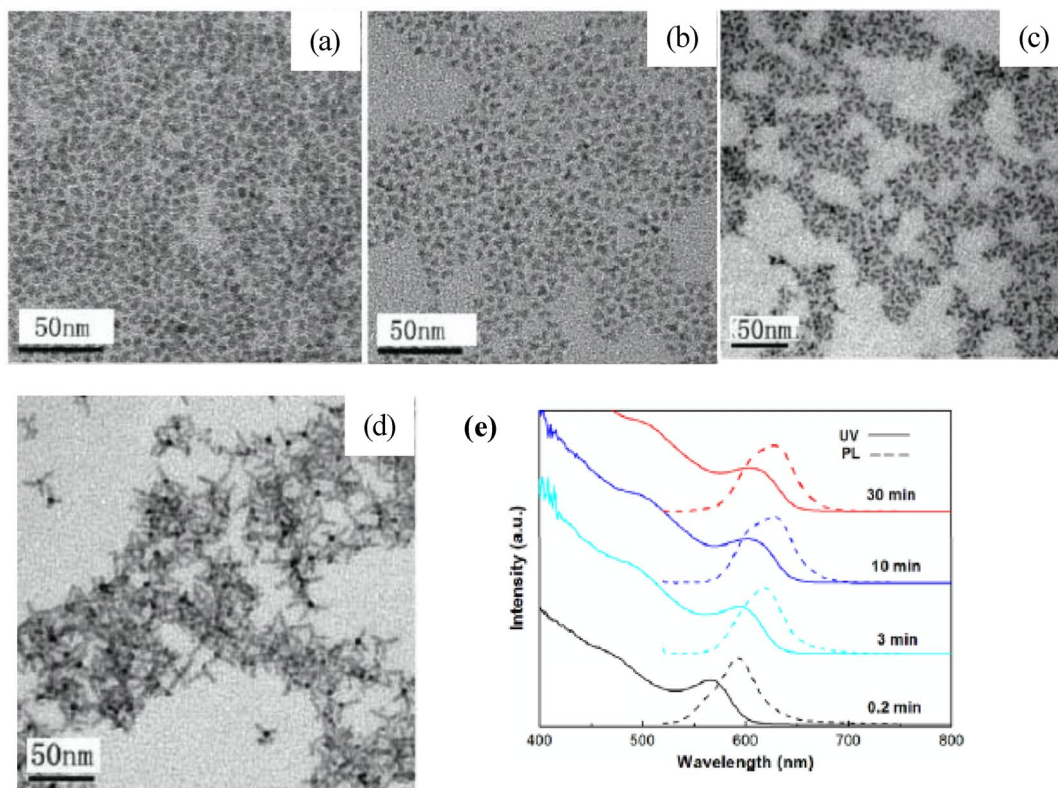
Fig. 2 The representative TEM images of four CdSe nanocrystals prepared with different reaction times: (a) 0.2 min, (b) 1 min, (c) 3 min, (d) 10 min, and (e) the temporal evolutions of UV and PL spectra of tetrapod-shaped CdSe nanocrystals. Reproduced from [23]. Copyright © 2011, IOP Publishing Ltd.

"BLINKING" EFFECT AND HYBRID PHOTOVOLTAIC APPLICATION OF CdSe NANO-TETRAPODS

As far as we know, systemic research on the optical and electric properties of CdSe nano-tetrapods is really scarce [24,25]. However, the applications of CdSe nano-tetrapods in hybrid photovoltaic devices have been widely studied. Researches show that CdSe nano-tetrapods have obvious advantages in the photovoltaic applications. In this part, an interesting phenomenon—"blinking"—observed from CdSe nano-tetrapods synthesized by the method in ref. [21] will be discussed firstly. Then the photovoltaic application of CdSe nano-tetrapods will be highlighted.

"BLINKING" EFFECT IN CdSe NANO-TETRAPODS

When excited by 400 nm pulse laser from a Ti:Sapphire laser, an interesting phenomenon is found from CdSe nano-tetrapods in chloroform solution at room temperature. Figure 3 shows the room-temperature PL spectrum of CdSe nano-tetrapods excited with 200 mW laser. As can be seen, there are some uniform small peaks existing in the broad PL peak. The illuminant point twinkles with a certain frequency. Here, we would like to borrow the noun "blinking" to describe this phenomenon of our samples. In our case, there are thousands of tetrapods in the solution contributing to the blinking. The typical intensity time trace of PL intermittency for tetrapod CdSe nanocrystals excited by various powers at room temperature are shown in Fig. 5a. The detected wavelength is fixed at 580 nm, which correspond to the maximum of PL peak. Figure 4a indicates that if the excitation power is low enough (i.e., 6 mW), no
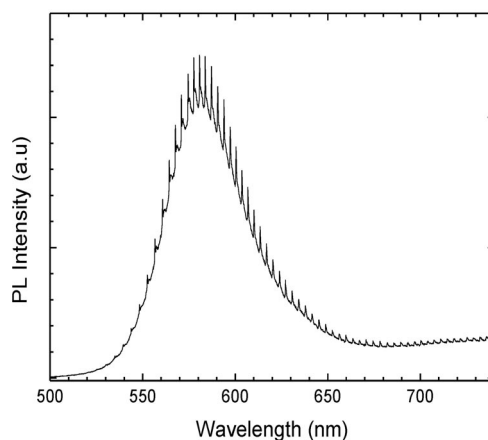
Fig. 3 Room-temperature PL spectrum of CdSe tetrapod sample; excitation power and wavelength are 200 mW and 400 nm, respectively.
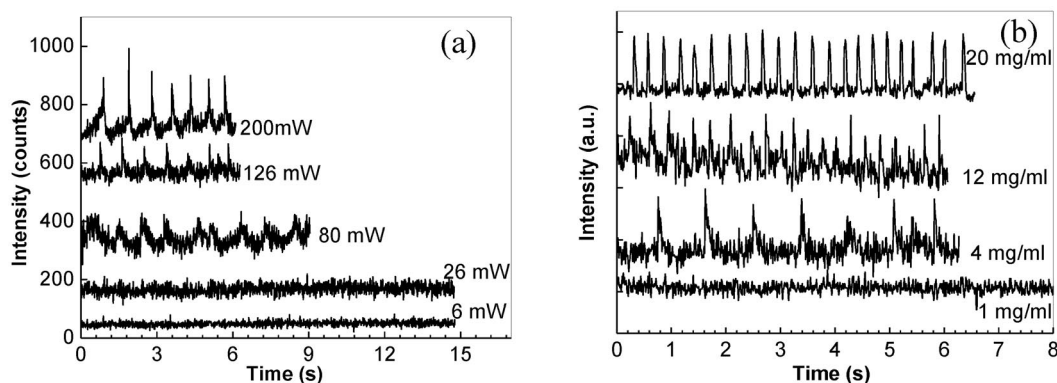

Fig. 4 (a) The typical intensity time trace of PL intermittency for CdSe tetrapods sample excited by various powers at room temperature; excitation wavelength is 400 nm. (b) The room-temperature "blinking" effects from CdSe tetrapods sample with different concentrations; excitation power and wavelength are 60 mW and 400 nm, respectively. In both spectra, the detected wavelength is fixed at 580 nm.

blinking is observed, while the blinking effect becomes more and more obvious as the excitation power increases. It indicates that the blinking effect may be related to the optic pressure and the thermal effect. The blinking effects from sample with different concentrations are also investigated, as shown in Fig. 4b. The excitation power is 60 mW, and the detected wavelength is 580 nm. It can be seen that as concentration increases, the blinking effect becomes more intensive and homogeneous. The blinking effect may even disappear if the solution is too dilute (i.e., 1 mg/ml), indicating that the blinking of our sample is from a big group of nanoparticles. Therefore, the noun "blinking" we used here is very different from that used in the literature, which is from a single particle as the other authors have observed [26,27]. The blinking effect is assumed to be related to the Brown movements of some clusters formed by these nanoparticles. However, the exact reason why the blinking effect can be observed from the solution samples is still not clear right now. More experiments and deep exploration are needed.

CdSe NANO-TETRAPODS BASED HYBRID PHOTOVOLTAIC DEVICES

Photovoltaic devices based on solution-processable conjugated polymers are attractive for the production of low-cost solar cells [28]. To obtain high efficiencies, it is necessary to have an interpenetrating network of electron- and hole-accepting components within the device. This can be achieved using polymer blends [29] or mixtures of conjugated polymers with C_{60} derivatives [30,31]. Nanocrystals of inorganic semiconductors such as CdSe also act as good electron acceptors from conjugated polymers; however, the efficiency of photovoltaic devices made with spherical nanocrystals is limited by problem of electron extraction through the nanocrystal network [32,33]. The use of nanorods instead of spherical nanocrystals has been shown to give significantly higher efficiencies because of the smaller number of interparticle hops necessary for electrons to leave the device [5,34]. However, nanorods have a tendency to lie in the plane of the film, which is not the optimum arrangement for electron extraction, and there is significant scope for improvement in efficiency by designing optimized microstructures. CdSe nano-tetrapods can provide improved electron transport perpendicular to the plane of the device, since unlike rods, they are unable to lie flat within the plane of the film.

Sun and co-workers fabricated photovoltaic devices from blends of TOPO-capped branched CdSe nanoparticles and a conjugated polymer [7]. It is found that these devices give improved performance compared with devices made from nanorod/polymer blends. The used CdSe nano-tetrapods and nanorods are shown in Figs. 5a,b, respectively. Photovoltaic devices are fabricated as shown in Fig. 5c. A blend of poly(3,4-ethylene dioxythiophene) with poly(styrene sulfonate) (PEDOT/PSS) is used as the anode and is spin-coated onto an oxygen-plasma-treated indium tin oxide (ITO) substrate.
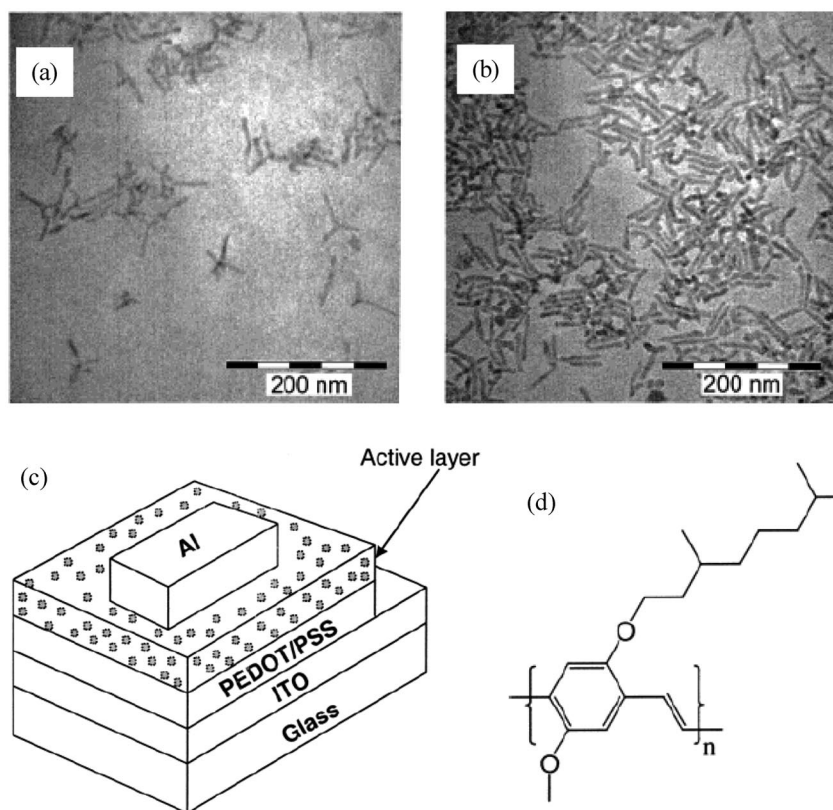

Fig. 5 TEM images of CdSe (a) nano-tetrapods and (b) nanorods. (c) Photovoltaic devices structure. (d) Chemical structure of OC_1C_{10}-PPV. Reproduced from [7]. Copyright © 2003, American Chemical Society.

The tetrapod or nanorod solution and poly[2-methoxy-5-(3', 7'-dimethyl-octyloxy)-*p*-phenylenevinylene] (OC_1C_{10}-PPV) solution are thoroughly mixed and spin-coated onto the surface of the PEDOT/PSS. Aluminum is used as the cathode which is deposited onto the active layer. Figure 5d shows the chemical structure of OC_1C_{10}-PPV. The short-circuit external quantum efficiency (*EQE*) action spectra for polymer/tetrapod and polymer/nanorod devices are shown in Fig. 6a. With CdSe tetrapods, the maximum short-circuit *EQE* is up to 45 % at 480 nm, which is almost a factor of 2 larger than that in the nanorod devices. Figure 6b shows the current density as a function of voltage for a polymer/tetrapod device under 0.39 mW cm^{-2} illumination at 480 nm. The short-circuit current density (I_{sc}), open-circuit voltage (V_{oc}), and fill factor (*FF*) are –0.069 mA cm^{-2}, 0.53 V and 0.49, respectively. The power conversion efficiency (η) is determined to be 4.5 %. Under illumination at AM 1.5 global conditions, the solar power conversion efficiency is 1.8 %, which is slightly higher than that of poly(3-hexylthiophene) (P3HT)/nanorod devices [5]. After two years, Sun et al. showed that the efficiency of polymer/CdSe tetrapods photovoltaic devices can be significantly improved by spin-coating the films from a high-boiling-point solvent such as 1,2,4-trichlorobenzene, which evaporates slowly instead of chloroform [35].
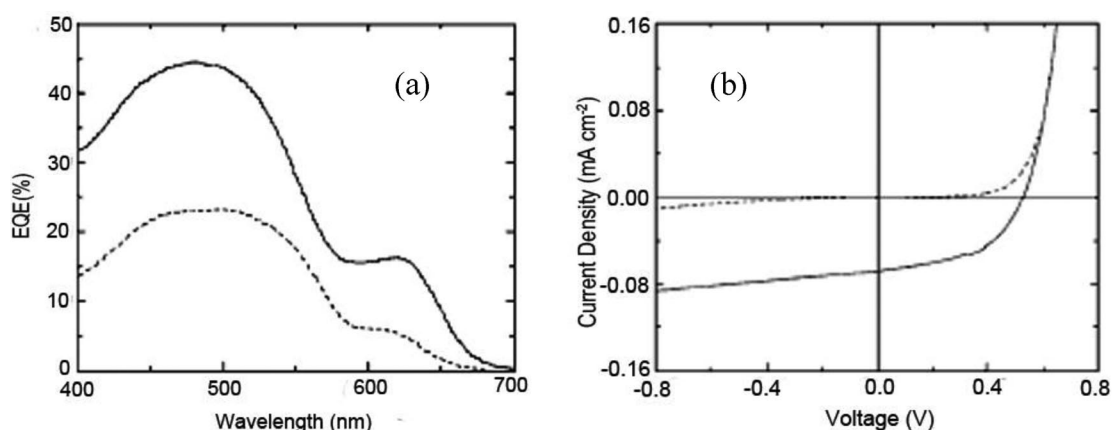

Fig. 6 (a) Short-circuit *EQE* action spectra of photovoltaic devices containing CdSe nanorods (dashed line) and tetrapods (solid line). (b) Current density vs. voltage for tetrapod/OC_1C_{10}-PPV device in the dark (dashed line) and under 0.39 mW cm^{-2} illumination at 480 nm. V_{oc} = 0.53 V, I_{sc} = –0.069 mA cm^{-2}, *FF* = 0.49, and η = 4.45 %. Reproduced from [7]. Copyright © 2003, American Chemical Society.

Recently, Kim's group used OA-capped tetrapod nanocrystals of CdSe, CdTe, and type II heterostructured CdTe/CdSe to investigate the effects of nanocrystal compositions and type II heterojunction on the photovoltaic properties of hybrid solar cells [36]. The hybrid solar cell based on the blend of CdSe nano-tetrapods and P3HT with a weight ratio of 6:1 shows the maximum power conversion efficiency of 1.03 % under AM 1.5 G condition, and the maximum short-circuit *EQE* is 43 % at 415 nm as indicated in Fig. 7, while CdTe and CdTe/CdSe heterojunction nano-tetrapods show relatively poor performance in the photovoltaic devices.
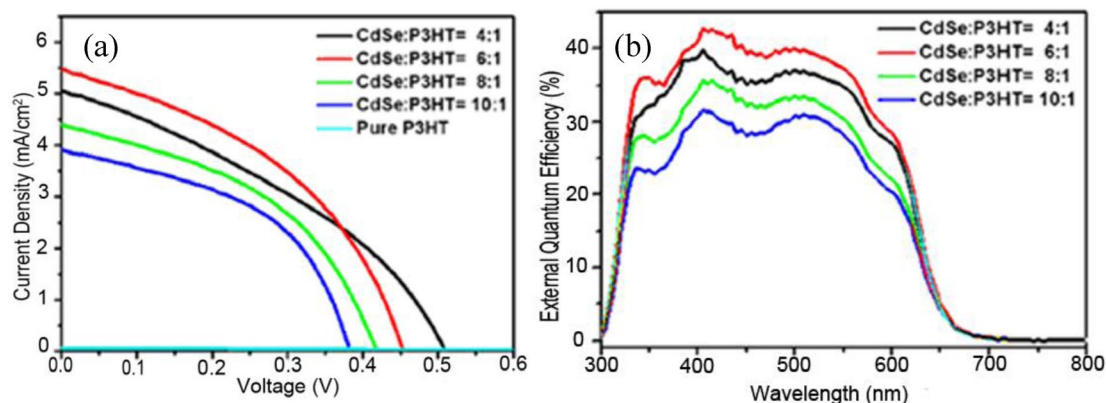
Fig. 7 The (a) *I–V* and (b) short-circuit *EQE* action spectra of hybrid solar cells based on the blend of CdSe nano-tetrapods and P3HT with different ratio (a layer thickness of about 144 nm). Reproduced from [33]. Copyright © 2011, Elsevier.

CONCLUSION AND OUTLOOK

Although the studies of CdSe nano-tetrapods were initiated just a few years ago, considerable progress has been made, which demonstrates that CdSe nano-tetrapods are amongst the most promising nano-structures under investigation. There is still considerable potential for future study of CdSe nano-tetrapods. For example, the interesting "blinking" effect observed from CdSe nano-tetrapods in solution is not yet clearly understood, and further work is necessary to determine its origin.

Applications of CdSe nano-tetrapods in the hybrid solar cells have been extensively investigated, and it was found that incorporation of CdSe nano-tetrapods can greatly improve the performance of hybrid photovoltaic devices. CdSe nano-tetrapods are now synthesized through colloidal nanosynthesis methods with TOPO or OA as the coordinate surfactant and TOPSe or TBPSe as Se precursor. Although about 95 % of the surface ligand is removed from the CdSe samples by washing the nanocrystals several times with different solvents, the residue TOPO or OA and TOP or TBP can still affect the electron transport of the CdSe nanocrystalline phase, which will decrease the power conversion efficiency of a hybrid solar cell [37]. So one of the key prerequisites for the successful utilization of CdSe nano-tetra-pod-based hybrid solar cells is to ensure that all traces of residual organic ligand and solvent are removed.

Lee and co-workers successfully synthesized type II CdTe/CdSe heterostructure tetrapod nanocrystals which were based on CdTe nano-tetrapods, and found that the prepared heterostructure nano-tetrapods have optical properties typical of type II heterostructures that are well suited for photovoltaic applications [38]. They also studied hybrid solar cells based on a blend of these heterostructures and P3HT. Although these devices showed relatively poorer performance than that of CdSe nano-tetra-pod-based hybrid solar cells, this investigation helped to understand the key factors that influence the performance of hybrid solar cells [36]. However, studies on CdSe tetrapod-based heterostructures and all-inorganic photovoltaic devices based on CdSe nano-tetrapods are limited. CdSe nano-tetrapods are attractive owing to the unique intrinsic characteristics of CdSe materials, the novel physical and chemical properties, and potential applications in solar cells. There still is a lot of room for future development in growth and applications of CdSe nano-tetrapods. It is believed that future research work in this area will further promote the understanding and applications of this nanostructure.

REFERENCES

1. L. Manna, D. J. Milliron, A. Meisel, E. C. Scher, A. P. Alivisatos. *Nat. Mater.* **2**, 382 (2003).
2. H. T. Liu, A. P. Alivisatos. *Nano Lett.* **4**, 2397 (2004).
3. D. L. Klein, R. Roth, A. K. L. Lim, A. P. Alivisatos, P. McEuen. *Nature* **389**, 699 (1997).
4. C. Wang, M. Shim, P. Guyott-Sionnest. *Science* **291**, 2390 (2001).
5. W. U. Huynh, J. J. Dittmer, A. P. Alivisatos. *Science* **295**, 2425 (2002).
6. W. K. Woo, K. T. Shimizu, M. V. Jarosz, R. G. Neuhauser, C. A. Leatherdale, M. A. Rubner, M. G. Bawendi. *Adv. Mater.* **14**, 1068 (2002).
7. B. Q. Sun, E. Marx, N. C. Greenham. *Nano Lett.* **3**, 961 (2003).
8. E. C. Scher, L. Manna, A. P. Alivisatos. *Philos. Trans. R. Soc. London, Ser. A* **361**, 241 (2003).
9. Y. Dai, Y. Zhang, Q. K. Li, C. W. Nan. *Chem. Phys. Lett.* **83–86**, 358 (2002).
10. H. Q. Yan, R. He, J. Pham, P. D. Yang. *Adv. Mater.* **15**, 402 (2003).
11. Y. W. Jun, S. M. Lee, N. J. Kang, J. Cheon. *J. Am. Chem. Soc.* **123**, 5150 (2001).
12. Y. W. Jun, Y. Y. Jung, J. Cheon. *J. Am. Chem. Soc.* **124**, 615 (2002).
13. M. Chen, Y. Xie, J. Lu, Y. J. Xiong, S. Y. Zhang, Y. T. Qian, X. M. Liu. *J. Mater. Chem.* **12**, 748 (2002).
14. W. W. Yu, Y. A. Wang, X. G. Peng. *Chem. Mater.* **15**, 4300 (2003).
15. X. S. Fang, U. K. Gautam, Y. Bando, B. Dierre, T. Sekiguchi, D. Golberg. *J. Phys. Chem. C* **112**, 4735 (2008).
16. X. S. Fang, Y. Bando, U. K. Gautam, T. Y. Zhai, H. B. Zeng, X. J. Xu, M. Y. Liao, D. Golberg. *Crit. Rev. Solid State Mater. Sci.* **34**, 190 (2009).
17. X. S. Fang, T. Y. Zhai, U. K. Gautam, L. Li, L. M. Wu, Y. Bando, D. Golberg. *Prog. Mater. Sci.* **56**, 175 (2011).
18. Z. A. Peng, X. G. Peng. *J. Am. Chem. Soc.* **124**, 3343 (2002).
19. L. Manna, E. C. Scher, A. P. Alivisatos. *J. Am. Chem. Soc.* **122**, 12700 (2000).
20. L. Manna, E. C. Scher, L. S. Li, A. P. Alivisatos. *J. Am. Chem. Soc.* **124**, 7136 (2002).
21. Q. Pang, L. J. Zhao, Y. Cai, D. P. Nguyen, N. Regnault, N. Wang, S. H. Yang, W. K. Ge, R. Ferreira, G. Bastard, J. N. Wang. *Chem. Mater.* **17**, 5263 (2005).
22. W. Y. L. Ko, H. G. Bagaria, S. Asokan, K. J. Lin, M. S. Wong. *J. Mater. Chem.* **20**, 2474 (2010).
23. H. M. Liu, H. Tao, T. B. Yang, L. B. Kong, D. H. Qin, J. Chen. *Nanotechnology* **22**, 045604 (2011).
24. L. J. Zhao, Q. Pang, S. H. Yang, W. K. Ge, J. N. Wang. *Phys. Lett. A* **373**, 2965 (2009).
25. L. J. Zhao, Q. Pang, S. H. Yang, W. K. Ge, J. N. Wang. *Appl. Phys. A* **103**, 279 (2011).
26. M. Nirmal, B. O. Dabbousi, M. G. Bawendi, J. J. Macklin, J. K. Trautman, T. D. Harris, L. E. Brus. *Nature* **383**, 802 (1996).
27. S. A. Empedocles, D. J. Norris, M. G. Bawendi. *Phys. Rev. Lett.* **77**, 3873 (1996).
28. J. Nelson. *Curr. Opin. Solid State Mater. Sci.* **6**, 87 (2002).
29. J. J. M. Halls, C. A. Walsh, N. C. Greenham, E. A. Marseglia, R. H. Friend, S. C. Moratti, A. B. Holmes. *Nature* **376**, 498 (1995).
30. G. Yu, J. Gao, J. C. Hummelen, F. Wudl, A. J. Heeger. *Science* **270**, 1789 (1995).
31. S. E. Shaheen, C. J. Brabec, N. S. Sariciftci, F. Padinger, T. Fromherz, J. C. Hummelen. *Appl. Phys. Lett.* **78**, 841 (2001).

32. N. C. Greenham, X. G. Peng, A. P. Alivisatos. *Phys. Rev. B* **54**, 17628 (1996).
33. D. S. Ginger, N. C. Greenham. *Phys. Rev. B* **59**, 10622 (1999).
34. W. U. Huynh, X. G. Peng, A. P. Alivisatos. *Adv. Mater.* **11**, 923 (1999).
35. B. Q. Sun, H. J. Snaith, A. S. Dhoot, S. Westenhoff, N. C. Greenham. *J. Appl. Phys.* **97**, 014914 (2005).
36. H. Lee, S. Kim, W. S. Chung, K. Kim, D. Kim. *Solar Energy Mater. Solar Cells* **95**, 446 (2011).
37. L. L. Han, D. H. Qin, X. Jiang, Y. S. Liu, L. Wang, J. W. Chen, Y. Cao. *Nanotechnology* **17**, 4736 (2006).
38. H. Lee, S. W. Yoon, J. P. Suh, J. S. Lee, H. Lim, D. Kim. *Solar Energy Mater. Solar Cells* **93**, 779 (2009).